4.1 SUMMARY OF RESULTS FOR CAI #1

To maintain a stable closed-loop servo system for angle tracking, the radar must maintain constant angle sensitivity independent of target size and range. The AGC circuit normalizes the radar input signal by applying to the IF amplifier stages a negative DC voltage that is proportional to the input signal voltage. Thus, as the input signal increases, the gains of the AGC controlled amplifier stages decrease. A block diagram of the AGC portion of a tracking radar receiver is shown in Figure 4.1-1.

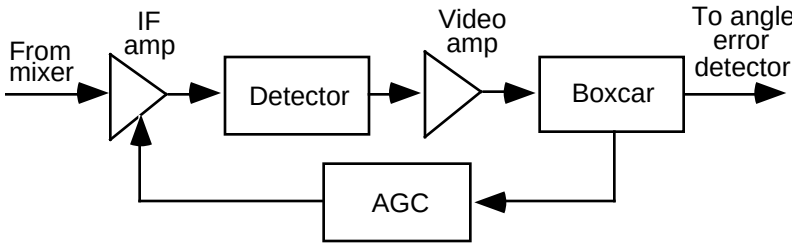

FIGURE 4.1-1. Tracking Radar Receiver.

In *RADGUNS*, variable *AGCSIG* is used to continuously control the IF amplifier gains. Comparison of *AGCSIG* to the control voltage measured during range test shows good correlation both graphically and numerically. Table 4.1-1 summarizes the results of this assessment.

TABLE 4.1-1. Validation Results for AGC.

Data Source	Major Conditions	Statistical MOEs	Results
Range Test - Giant Hawk	AAA system in autotrack	Graphical correlation	Close agreement
	mode against	Numerical correlation	≥ 0.678
	a non-	Standard deviation	Good agreement
	maneuvering	Range of voltages	Good agreement
	B-1B, no ECM	Mann-Whitney U test	Within 95% confidence interval in 3 out of 4 cases

The receiver output is the input to the target tracker; therefore, this assessment feeds the target tracking CAI (see Section 4.2).

4.1.1 Assessment – Case 1

Assessment Description

Test Data Description. The Giant Hawk Test is described in Section 4.2 under Assessment Description – B-1B. Table 4.1-2 lists the direction of aircraft travel, the offset from the threat, the direction of the offset, and the average altitude and speed of the aircraft. Table 4.1-3 shows the data fields used in this analysis. All data were collected at ten samples per second.

TABLE 4.1-2. B-1B Test Matrix.

Pass	Type	Direction	Offset (m)	Offset Direction	Altitude (m)	Speed (m)
2	Linear	SE/NW	734	SW	223	277
13	Linear	NW/SE	33	NW	571	281
14	Linear	SE/NW	904	SW	499	274

TABLE 4.1-3. B-1B Data Fields.

Field	Description
REF_X_POS REF_Y_POS REF_Z_POS	TSPI tracker's aircraft position rotated to the threat's location, where positive x is east, positive y is north, and positive z is up
REF_XVEL REF_YVEL REF_ZVEL	X-, y-, and z-components of the aircraft velocity rotated to the threat's location
MTAZ_0 MTEL_0 MTRG_0	Threat's azimuth, elevation, and range tracking modes
VIC_AGC_MN	Threat's continuous AGC voltage

Only autotrack portions of each engagement were analyzed. During pass 13, the angular rate limits of the tracker were exceeded causing the system to break lock as the aircraft flew overhead. Pass 13 is therefore broken into inbound and outbound autotracking sections. The MTI switch remained in the "OFF" position for all three passes.

Validation Methodology. The reference tracker's x, y, and z aircraft positions were used to generate BLUMAX flight paths for input to *RADGUNS*. *RADGUNS* v.1.9 was executed with the following input conditions:

Model Mode:	SINGL/RADAR
Target Type:	B-1B
Flight Path:	BLUMAX
Radar type:	RAD1
MTI mode:	OFF
Clutter/Multipath:	None
Outputs:	AGC voltage (variable *AGCSIG*)

The model output AGC voltage was compared to the measured AGC voltage both graphically and statistically. Comparison of the modeled and measured means for each of the three passes revealed a constant bias that was accounted for by applying a constant gain of –5.9 to the measured AGC voltage. Standard deviation, range of voltages, correlation

coefficient, and the non-parametric Mann-Whitney U test with a 95% confidence interval were used as statistical MOEs.

Results

Flight paths for each of the three passes are shown in Appendix A, Figures A-1, A-3, and A-5. Figures 4.1-2 through 4.1-4 show both the measured (adjusted) and modeled AGC voltage versus time. In each case, the AGC voltage increases as the input voltage increases (target range decreases). The model predicts the general shape of the curve, however, the peak voltage of the system is lower than the modeled peak in all cases, and the model does not predict the jitter that is inherent in the measured voltage. Figures 4.1-2 through 4.1-4 show both the modeled voltage and the smoothed system voltage. The smoothed voltage is the result of a moving average over 20 samples (2 s).

Applying a gain factor to the system data effectively changes the mean value of the data, however, other statistics such as standard deviation, range of voltages, and correlation coefficient are still useful in comparing model voltages to system voltages. In addition, the Mann-Whitney U Test is useful for determining if the two data sets come from the same population. For a confidence interval of 95%, it may be assumed that the two sets are drawn from the same population if the calculated Z value falls between in Table 4.1-4.

TABLE 4.1-4. AGC Voltage Statistics.

Pass	RADGUNS σ as % of Mean	SYSTEM σ as % of Mean	RADGUNS Range (V)	SYSTEM Range (V)	Correlation Coefficient	Z Value
2	48	41	38.57	30.90	0.944	-0.507
13 in	41	38	24.1	27.00	0.900	0.568
13 out	27	39	7.36	18.74	0.678	10.211
14	46	38	35.81	31.05	0.858	0.180

RADGUNS exhibits a higher standard deviation of voltages for passes 2, 14, and the inbound portion of pass 13 that is caused by the higher peak voltage in the model. This peak voltage also increases the range of voltages in the model. For the outbound portion of pass 13 where the AGC voltage does not approach the peak, the system shows a greater standard deviation of voltages caused by the apparent fluctuation in AGC voltage over time. It is hard to determine without further characterization of the AGC circuit whether this fluctuation is a true phenomenon in the system or noise introduced or amplified by instrumentation. In passes 2, 14, and the inbound portion of 13, the correlation coefficient is high indicating a strong linear association between measured and modeled voltages. The Z value calculated for these three cases is well within the critical range, and it can be assumed that the modeled and measured voltages are drawn from the same population. Additional adjustment of the mean system voltage would improve the correlation coefficient and Z value for the outbound portion of pass 13.

Conclusions

The results of this assessment indicate that *RADGUNS* simulates the AGC functional element reasonably well. For a large target at close range, the model produces AGC voltages higher than those measured from the system. This will cause lower gains in the

modeled AGC controlled IF amplifier stages and smaller error inputs to the track loop. At greater ranges, however, the model closely simulates the measured AGC voltage.

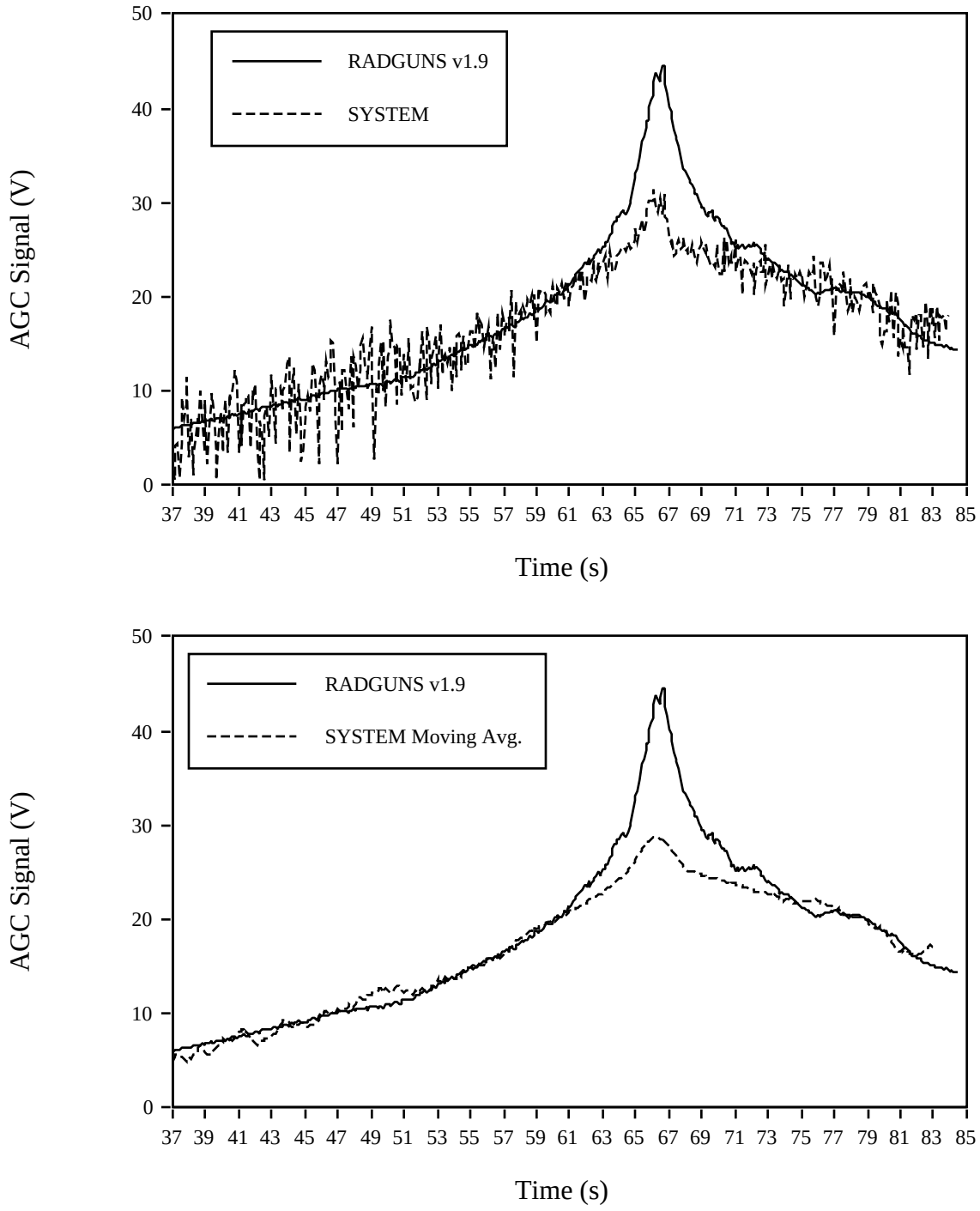

FIGURE 4.1-2. Measured and Modeled AGC for B-1B, Pass 2.

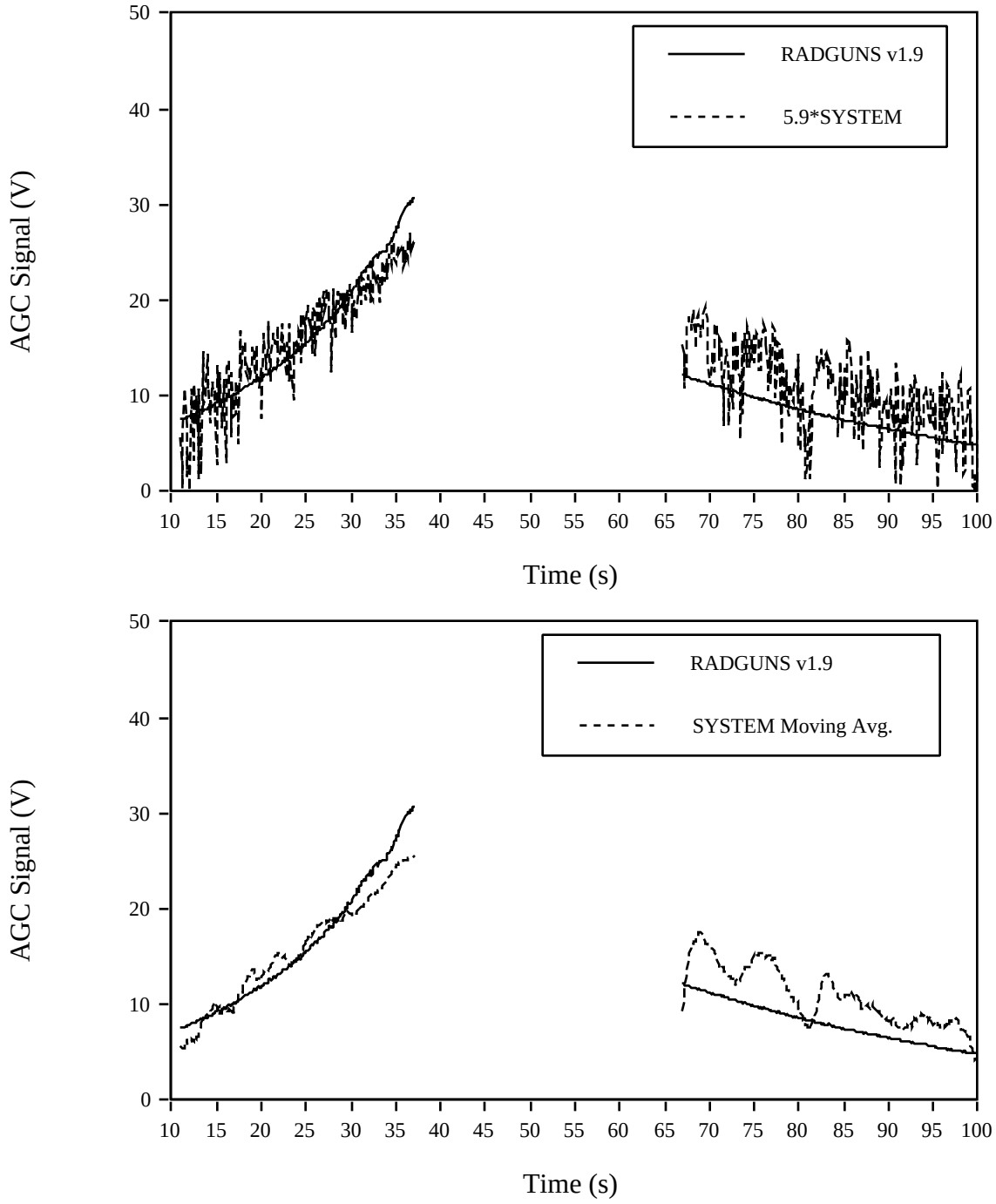

FIGURE 4.1-3. Measured and Modeled AGC for B-1B, Pass 13.

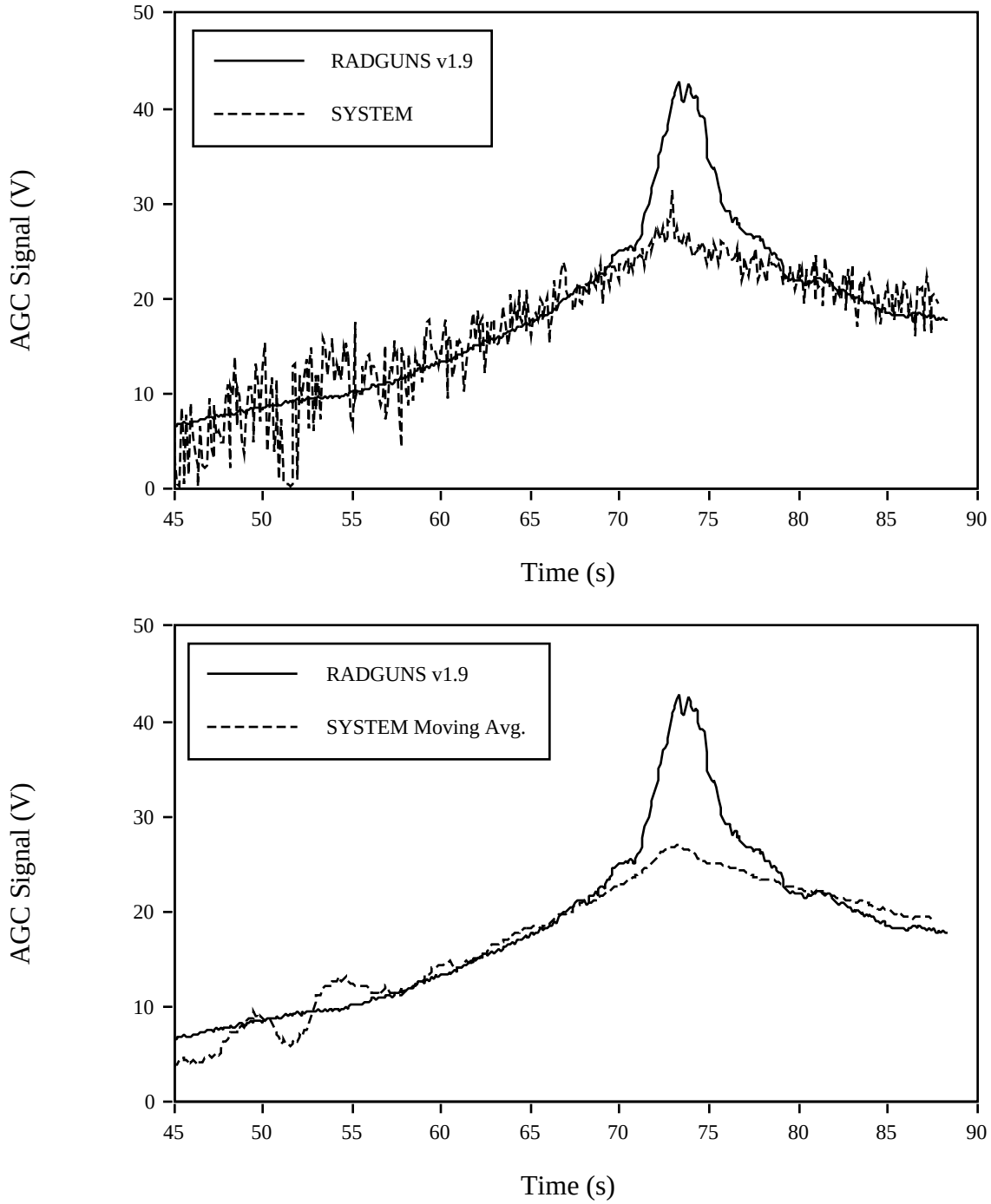

FIGURE 4.1-4. Measured and Modeled AGC for B-1B, Pass 14.